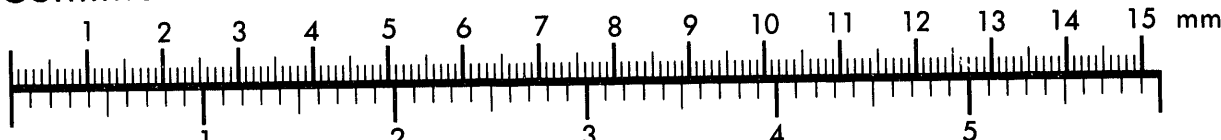




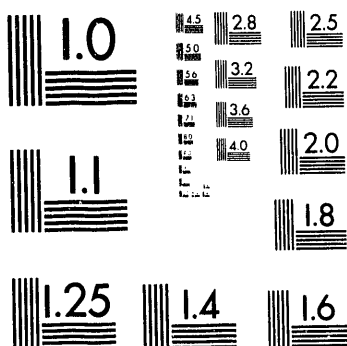
Association for Information and Image Management

1100 Wayne Avenue, Suite 1100
Silver Spring, Maryland 20910
301/587-8202

Centimeter



Inches



MANUFACTURED TO AIIM STANDARDS
BY APPLIED IMAGE, INC.

1 of 1

Los Alamos National Laboratory is operated by the University of California for the United States Department of Energy under contract W-7405-ENG-36.

PC
JUN 04 1993
COPY

TITLE: GENERATION AND FOCUSING OF HIGH ENERGY, 35-kA ELECTRON BEAMS
FOR PULSED-DIODE RADIOGRAPHIC MACHINES: THEORY AND
EXPERIMENT

AUTHOR(S): R. L. Carlson, M. J. George, T. P. Hughes, D. R. Welch

SUBMITTED TO: 1993 Particle Accelerator Conference
Washington, DC
May 17-20, 1993

By acceptance of this article, the publisher recognizes that the U.S. Government retains a nonexclusive, royalty-free license to publish or reproduce the published form of this contribution, or to allow others to do so, for U.S. Government purposes.

The Los Alamos National Laboratory requests that the publisher identify this article as work performed under the auspices of the U.S. Department of Energy.

Los Alamos

MASTER

Los Alamos National Laboratory
Los Alamos, New Mexico 87545

DISTRIBUTION OF THIS DOCUMENT IS UNLIMITED
EB

Generation and Focusing of High Energy, 35-kA Electron Beams for Pulsed-Diode Radiographic Machines: Theory and Experiment*

R.L. Carlson and M.J. George
Los Alamos National Laboratory
P.O. Box 1663
Los Alamos, NM 87545
and
T.P. Hughes and D.R. Welch
Mission Research Corp.
1720 Randolph Road SE
Albuquerque, NM 87108

Abstract

Cathode ball and anode planar-foil geometries used to generate self-focused beams onto x-ray conversion targets via beam-induced ionization in gas cells have been investigated since the early 1970's by J. C. Martin et al at Aldermaston, U.K. The building of a succession of increasingly higher voltage, pulsed-diode machines tailored for flash x radiography has resulted. Given sufficient dose to penetrate an object, the spot size of the x-ray source generally determines the resolution of a radiograph. Reported are particle-in-cell code simulations applied to beam generation in the A-K gap and the self-focusing onto the target. A Monte Carlo code for neutron, photon, and electron transport converts the beam particles at the target to photons with transport to a film plane used to calculate the spot size. Comparisons are made to experiments using the Ector (3.5-4 MeV) and PIXY (4-8 MeV) pulsed-diode radiographic machines at Los Alamos.

of the ball is painted with silver to aid in the start of explosive cold cathode emission. The resultant 3.5-4 MeV electrons are accelerated across the 13-mm A-K gap and impinge upon a 25- μ m aluminum-foil anode. Figure 2 shows an average of five shots using a 200-MHz digitizer to record the voltage across the axial insulator stack and the diode current.

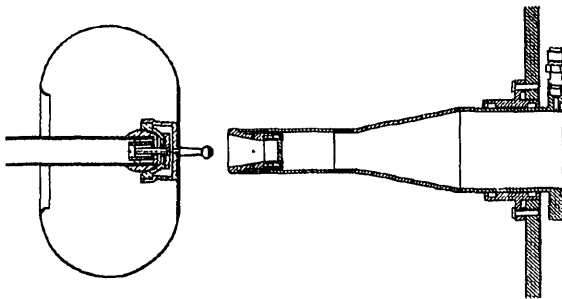


Figure 1. Ector Diode Region.

I. INTRODUCTION

The study of explosively driven systems at Los Alamos has been enhanced since the mid-1960's by flash radiography [1], a technique in which a pulsed beam of electrons interacts with a converter target to produce x-rays that penetrate an object and are detected and recorded by a film pack. Pulsed power diodes, such as Mogul-D attributed to J.C. Martin and his colleagues, can produce high doses (240 R/pulse at 1 m with collimation), energies of 8 MeV, and reasonably small spot sizes (7-mm diam) [2,3]. Although a variety of machines with differing energy, dose, and spot size have been and are continuing to be built, all figures of merit emphasize the importance of a small spot size for high resolution flash radiography [4,5].

Figure 1 shows the anode-cathode (A-K) region of the Ector pulsed diode machine at Los Alamos. This machine (formerly Mogul C) was originally built in the 1960's at Aldermaston and shipped to Los Alamos in 1981. The output of a Blumlein feeds a magnetically insulated transmission line stalk that terminates in a field-shaping electrode or "beam stopper". The cathode consists of a 12.7-mm-diam polished stainless steel ball on an 18-mm stem; the frontal area (90%)

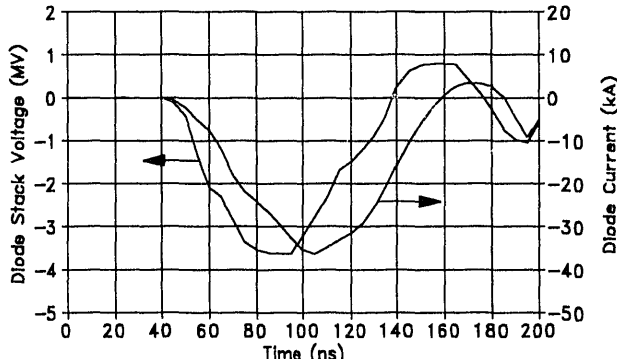


Figure 2. Ector Stack Voltage and Diode Current.

The beam then encounters a low pressure (typically 0.8 to 1.2 torr) drift section of air where direct impact ionization of the gas results in electrons and ions. The electrons, being light and mobile, are repelled by the beam leaving behind a region of positive charge that cancels out the beam's self-radial electric field. The beam's high current (~35 kA) together with the plasma return current create a net self-magnetic field that focuses the beam over a drift distance of 45 mm onto the x-ray conversion target with a spot size of 9- to 10-mm diam. The x-ray spot size is a time-integrated value and includes any beam motion in the focal plane.

*Work performed under the auspices of the U.S. Department of Energy.

II. THEORY AND EXPERIMENT

Figure 3 shows the results of a SPEED [6] calculation that gives the equipotential contours and electron trajectories for the 13-mm A-K gap of Ector at 3.5 MeV and 33.8 kA. The total current is reduced to 27.2 kA by limiting the emission to the 90% frontal area of the cathode ball; conversely, at fields above 800 kV/cm the rear of the ball and part of the stem would also emit, raising the total current to 36.0 kA. In all cases, it is presumed that the silver paint enhances the initial area of emission which is elsewhere suppressed by the lower fields and highly polished rear area of the ball and stem.

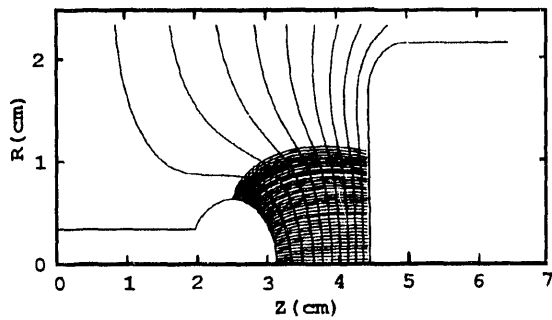


Figure 3. Ector at 3.5 MV with 13-mm A-K gap.

The output of SPEED is then post-processed to include the effects of scatter by the 25- μ m aluminum-foil anode and then input to the IPROP [7] PIC code. IPROP models gas conductivity generated by direct impact and secondary ionization and uses a semi-implicit electromagnetic field solver. The simulation for Ector is shown in Fig. 4.

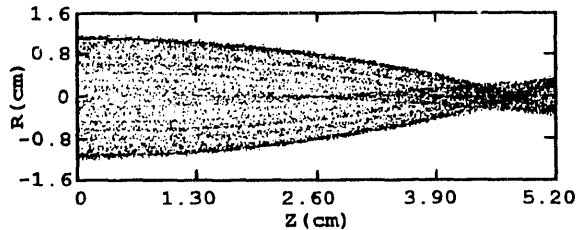


Figure 4. Transport in Ector Gas Cell at 1.2 Torr Air.

At lower energies the beam is divergent and larger in diameter at the foil which results in a longer focal length. At constant beam energy, a wider A-K gap (lower field on the ball) or a smaller cathode (reduced area of beam emission) produces much the same result. The beam at the target ($z=45$ mm) is 2.2-mm diam (rms). How does this compare to the radiographic spot size of Ector, which is about 9-mm diam? A similar question arose from the predictions [8] of IPROP and the measured 7-mm-diam spot size of Mogul D at 8 MeV during the design of the Los Alamos 8-MeV PIXY machine [9]. After optimizing the diode geometry, the radiographic spot size of PIXY was measured to be 9.5 ± 0.6 -mm diam for 18 shots at Ector voltages (3.5-4 MV) and A-K gaps of 12-, 13-, and 14-mm. It was anticipated that the measured spot size

would be smaller than Ector's in light of the IPROP predictions and the more trapezoidal voltage and current pulse of PIXY vs the half-sine-like pulse of Ector (Fig. 2).

SPEED and IPROP were next used to make detailed time-dependent calculations of the beam transport to the target. For this case, the driving voltage pulse of Ector was approximated as a half-sine having a base width of 85 ns and a peak of 3.5 MV. The beam's rms radius vs axial position in the drift cell is shown in Fig. 5 for the first 75 ns of the 85-ns pulse in successive time slices of 8.33 ns. The focus of the beam moves from past the target ($z=45$ mm) to a minimum value on the target of 2.2-mm diam (rms) at 33.3 ns; this is the same instantaneous condition as calculated in Fig. 4. At later times, the focus continues to move away from the target and toward the anode foil.

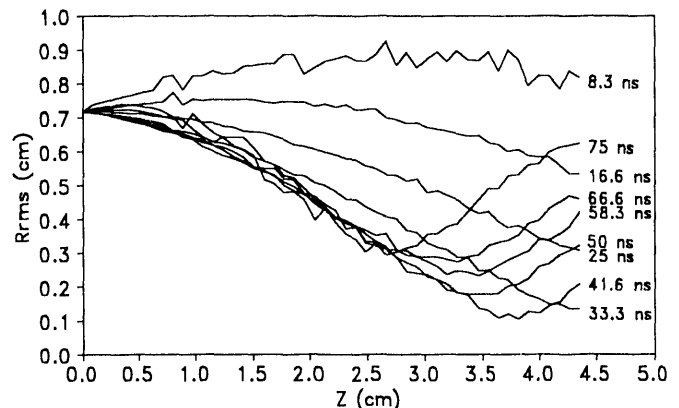


Figure 5. Beam Radius vs Axial Distance in Gas Cell.

Figure 6 shows the corresponding calculation of the beam and net current versus time in the 1.2-torr drift cell. At early time, the beam rapidly ionizes the gas and drives radial and axial return currents in the drift space. When high conductivity is reached, the net current (beam current minus plasma return current) increases slowly with time until the beam current drops below the net current. This continued increase in net current causes the self-magnetic field for focusing to increase with time. Figure 5 shows that the focal plane of the beam moves from past, through, and finally in front of the target. This is contrary to the expectation that the focal plane of the beam would move toward and past the target as the beam current and voltage drop late in time. The inductive nature of the plasma and the experimentally verified behavior of the net current [8] suggest that the temporal evolution of the net current is somewhat independent of the driving voltage and resulting beam current pulse shape. This effect could explain why the spot-size results obtained with the trapezoidal pulse of PIXY were essentially the same as those obtained with the sinusoidal-like pulse of Ector. The time-integrated electron beam size on the target of Fig. 5 is 5.4-mm-diam (rms).

To quantify the relationship between the electron beam distribution and the radiographic spot-size at the target, each particle from the output of IPROP was dose-weighted. The dose-weighting factor used was the 2.8 power of the voltage

multiplied by the charge of the particle. This calculation gives a dose distribution versus radius which is then converted to the radiographic spot size [3,5]. The results are spot sizes of 7.1- and 2.7-mm diam for the time-integrated and instantaneous cases of Fig. 5, respectively.

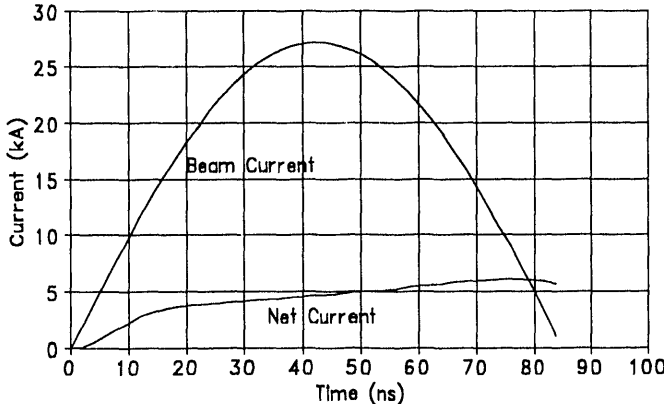


Figure 6. Beam and Net Current for Fig. 5 Simulation.

Although the above computed spot size is in close agreement with the measured results, it does not include the electron and photon transport processes that occur in the x-ray converter. The momentum and position of each particle from IPROP was used as an input to the MCNP [10] code to convert each particle at the 0.5-mm-thick tungsten target to photons. These photons were then transported to a film plane to calculate the radiographic spot size via an edge-projection technique [3]. To improve the photon statistics, two sets of source particles from IPROP ($\sim 10^3$ in the first set averaged over 1 ns centered at 33.3 ns, and $\sim 8 \times 10^4$ in the second set time-averaged over the 85-ns pulse) were replicated with azimuthal symmetry in the plane of the target. This technique increased the number of particles input to MCNP by 500-fold for the 1-ns and 10-fold for the 85-ns cases. Figure 7 shows the computed step-responses across an opaque edge as projected onto a film plane with a source magnification of 5 for the two data sets. The radiographic spot sizes are 3.15- and 7.44-mm diam for the near-instantaneous and time-integrated cases, respectively.

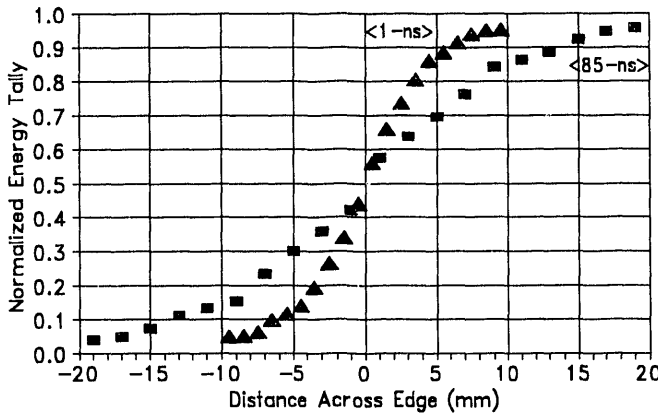


Figure 7. Edge Step-Responses via MCNP in Film-Plane.

III. CONCLUSION

Several codes, used in tandem, have modeled the beam generation, transport, gas-cell focusing, and x-ray conversion for a class of pulsed diode machines dedicated to flash x-radiography. The major parameters that control the focused size of the electron beam and its relationship to the radiographic spot size have been studied. The spot size is dominated by time-dependent motion of the beam's focal plane and not the emittance, foil scatter, nor the non linear forces that focus the beam. This movement is due to the temporal behavior of the net current, which appears to be independent of the voltage or current pulse shape. This motion might be minimized by using a shorter pulse length or tailoring the voltage to rise during the pulse. There is good agreement between either the dose-weighted (7.1-mm diam) or the MCNP (7.44-mm diam) methods and the measured 9.5-mm-diam spot sizes. The SPEED and IPROP codes along with the simpler dose-weighted method can be used to predict and guide improvement efforts for various machines.

IV. REFERENCES

- [1] T.J. Boyd, Jr., B.T. Rogers, F.R. Tesche, and Douglas Venable, "PHERMEX - A High-Current Electron Accelerator for Use in Dynamic Radiography," *Rev. Sci. Instr.* 36 (10), October 1965, pp. 1401-1407.
- [2] Private Communication with Mike Goodman of AWE, Aldermaston, U.K. and K.H. Mueller of Los Alamos.
- [3] K.H. Mueller, "Measurement and Characterization of X-Ray Spot Size," *Proceedings of the 1989 Flash Radiography Topical, American Defense Preparedness Association*, pp. 383-394.
- [4] J.C. Martin, "Aids to Estimating the Quality of Flash Radiographs," British Note SSWA/JCM/788/266, AWRE, Aldermaston, United Kingdom, August 1978.
- [5] J.C. Dainty and R. Shaw, *Image Science*, Academic Press Inc., New York, 1974.
- [6] SPEED was written by Jack Boers, Thunderbird Simulation, Inc.
- [7] M.M. Campbell, B.B. Godfrey, and D.R. Welch, "IPROP User's Manual: Post-processor Version," MRC/ABQ-R-1397, Mission Research Corporation, March 1991.
- [8] M.A. Mostrom, M.M. Campbell, R.M. Clark, and L.A. Wright, "Electron Focusing in the Neutral Gas Drift Tube," MRC/ABQ-R-1197, Mission Research Corporation, August 1989.
- [9] R.A. Lucht and S. Eckhouse, "Intense X-Ray Machine for Penetrating Radiography," *Proceedings of the 1989 Flash Radiography Topical, American Defense Preparedness Association*, pp. 333-346.
- [10] J.F. Briesmeister, ed., "MCNP: A General Monte-Carlo Code for Neutron and Photon Transport, Version 3A," LA-7396-M, Revision 2, (Version 4 includes electrons), Los Alamos National Laboratory, September 1986,

**DATE
FILMED**

8 / 18 / 93

END

